However, unlike the linear prediction procedure, no 'fast' algorithm exists for the solution of the involved equations, and thus the choise of procedure must depend on the complexity of the NMR spectrum, and on the available computational possibilities. Still, unbiased estimates of the spectral parameters I_j, ν_j, R_{2j}^*, and ϕ_j can be obtained with both methods, because both include a least-squares calculation based on equation (3).

5 CONCLUSION

The spectral methods described in this article (extrapolation of the FID by linear prediction, quantitative linear prediction, and least-squares FT) have all proved to be very useful in NMR spectroscopy. The major drawbacks of these methods have been the extensive computing time required and the need for very large amounts of computer memory. However, the new 'fast' algorithms together with the substantial improvements in minicomputers have reduced these drawbacks considerably, and made the use of linear prediction and least-squares analyses feasible on standard computational equipment that is normally available in NMR laboratories today.

6 RELATED ARTICLES

Fourier Transform Spectroscopy; Multidimensional Spectroscopy: Concepts.

7 REFERENCES

1. E. O. Brigham, 'The Fast Fourier Transform', Prentice-Hall, Englewood Cliffs, NJ, 1974, p. 85.
2. H. Gesmar, J. J. Led, and F. Abildgaard, *Prog. NMR Spectrosc.*, 1990, **22**, 255.
3. H. Barkhuijsen, R. de Beer, W. M. M. J. Bovée, and D. van Ormondt, *J. Magn. Reson.*, 1985, **61**, 465.
4. J. J. Led and H. Gesmar, *Chem. Rev.*, 1991, **91**, 1413.
5. S. M. Kay and S. L. Marple, Jr., *Proc. IEEE*, 1981, **69**, 1380.
6. J. Tang and R. Norris, *J. Magn. Reson.*, 1986, **69**, 180.
7. R. Kumaresan *IEEE Trans. ASSP*, 1983, **31**, 217.
8. D. Marion and A. Bax, *J. Magn. Reson.*, 1989, **83**, 205.
9. C. F. Tirendi and J. F. Martin, *J. Magn. Reson.*, 1989, **81**, 577.
10. E. T. Olejniczak and H. L. Eaton, *J. Magn. Reson.*, 1990, **87**, 628.
11. G. Zhu and A. Bax, *J. Magn. Reson.*, 1990, **90**, 405.
12. G. R. B. Prony, *J. L'Ecol Polytech. Paris*, 1795, **1**, 24.
13. R. Kumaresan and D. W. Tufts *IEEE Trans. ASSP*, 1982, **30**, 833.
14. H. Barkhuijsen, R. van de Beer, and D. van Ormondt, *J. Magn. Reson.*, 1986, **67**, 371.
15. H. Gesmar and J. J. Led, *J. Magn. Reson.*, 1988, **76**, 183.
16. J. Tang, C. P. Lin, M. K. Bowman, and J. R. Norris, *J. Magn. Reson.*, 1985, **62**, 167.
17. W. W. F. Pijnappel, A. van den Boogaart, R. de Beer, and D. van Ormondt, *J. Magn. Reson.*, 1992, **97**, 122.
18. H. Gesmar and P. C. Hansen, *J. Magn. Reson.*, 1994, **106**, 236.
19. H. Gesmar and J. J. Led, *J. Magn. Reson.*, 1989, **83**, 53.
20. F. Abildgaard, H. Gesmar, and J. J. Led, *J. Magn. Reson.*, 1988, **79**, 78.
21. R. Kumaresan, C. S. Ramalingam, and D. van Ormondt, *J. Magn. Reson.*, 1990, **89**, 562.

For list of General Abbreviations see end-papers

Biographical Sketches

Jens J. Led. *b* 1938. M.S. (chemistry), The Technical University of Denmark, 1963. Ph.D., 1968, Sc.D., 1988, University of Copenhagen. Faculty in Chemistry, University of Copenhagen, 1969–present. Visiting research associate, University of Utah, 1971–73. Approx. 60 publications. Current research specialties: NMR studies of protein structure and function, NMR signal analysis.

Henrik Gesmar. *b* 1948. M.S. (chemistry), B.A. (Spanish), 1983, Ph.D. (chemistry), 1988, University of Copenhagen. Faculty in Chemistry, University of Copenhagen, 1988–present. Approx. 25 publications. Primary research interest: NMR studies of proteins, with focus on spectral analysis and computational methods.

Fourier Transform Spectroscopy

Weston A. Anderson
Varian Associates, Palo Alto, CA, USA

---

1 INTRODUCTION

Fourier transform (FT) spectroscopy employs wideband excitation to simulate simultaneously all the transition lines of a nuclear magnetic resonance (NMR) spectrum to produce a time-dependent response signal. An FT is applied to the response signal and produces an NMR spectrum. The FT is a mathematical process for converting a signal that is a function of time to one that is a function of frequency.

The wideband excitation may be produced by several different methods, the most common in use today being pulsing of the applied radiofrequency (rf) field. Another method is modulating an rf by a random or pseudorandom noise source. Wideband sources with almost any spectral distribution may be generated using modern pulse programmers and frequency synthesizers controlled by digital logic. A method related to FT spectroscopy uses a very rapid scan of the rf source through the NMR spectral region.

In the pulsed NMR method, the time-dependent NMR response, called the free induction decay (FID), is sampled at uniform time intervals after the termination of the rf pulse. Each time sample is digitized and stored in a digital memory. To improve the sensitivity, the experiment may be repeated, the responses of subsequent pulses sampled at the same uniform time intervals, and the digitized values of each sample added to the value previously stored for the corresponding time interval. When a sufficient number of samples have been stored, the FT is applied, yielding an output spectrum that is a function of frequency. The advantage of FT NMR spectroscopy is the gain in sensitivity that can be obtained. For ^{1}H or ^{13}C NMR in liquid samples the gain can exceed a factor of 100.

2 HISTORICAL BACKGROUND

The FT is named after the French mathematician Jean Baptiste Joseph Fourier (1768–1830). Fourier taught at the École Normale in Paris when it opened in 1795, and later at the École Polytechnique. In 1801 he became Prefect of Isère, based at Grenoble. Here he investigated heat conduction, and in 1807 announced his use of a series of sines and cosines of integral multiples of a variable to represent almost any function. This idea originated in the works of Leonhard Euler (1707–83) and Daniel Bernoulli (1700–82). In 1816, Fourier moved to Paris, and in 1817 was made a Member of the French Academy of Science. In 1822 he published *Théorie Analytique de la Chaleur* in which he fully developed the theory and mathematics of the series now known by his name.

Spectroscopy started with optical spectroscopy, the dispersing of light into its spectral components or colors. In 1607, Isaac Newton illustrated that a beam of light, after passing through a glass prism, forms an elongated multicolored image called a spectrum. In 1802, Thomas Young developed the wave theory of light and related color to wavelength. In 1859, G. R. Kirchoff set out the general law connecting absorption and emission of light and showed that each species of atom has a uniquely characteristic spectrum. In 1881, A. A. Michelson invented the interferometer and used it to measure accurately the wavelengths of a number of atomic emission lines relative to the standard meter. In his monograph of 1907, Michelson explained the connection between the spectral pattern of a light beam and the corresponding time domain signals, i.e. that one can be derived from the other through an FT.[1] The Michelson optical interferometer made possible multiplex spectrometry, i.e. recording of all the spectral intervals simultaneously. The full power of this technique for increasing the sensitivity of infrared spectrometry was pointed out by Fellgett in 1951[2] and is known as the 'Fellgett advantage' or 'multiplex advantage'. The technique is unsuitable for NMR, however, because of the much longer wavelengths of NMR spectral frequencies.

NMR spectroscopy began with the discovery of the technique by Purcell and co-workers at Harvard[3] and Bloch and coworkers at Stanford,[4] reported early in 1946. The method used to obtain a spectrum was either to scan slowly the driving rf or the polarizing magnetic field strength. The resulting resonance could be displayed on an oscilloscope or on a strip chart recorder. This slow passage or continuous wave (CW) method was used for the first 20 years of NMR spectroscopy.

Some of the concepts of pulsed NMR were contained in the introductory section of Bloch's first detailed paper about NMR:[5]

> Not only a weak rf field, acting at resonance over very many Larmor periods, can produce an appreciable nuclear change of orientation, but also a strong field pulse, acting over only a few periods. Once the nuclear moments have been turned into an angle with the constant field, they will continue to precess around it and likewise cause a nuclear induction to occur at an instant when the driving pulse has already disappeared. It seems perfectly feasible to receive thus an induced nuclear signal of radiofrequency well above the thermal noise of a narrow band receiver.

The transient signal described here became known as the FID. Bloch did not specifically treat this case in the remainder of his paper. The concept appears to be covered by some of the broad claims of the Bloch–Hansen patent;[6] however, no specific application is shown that makes use of this technique.

Transient effects, commonly called 'wiggles', were observed in many of the early experiments. They occur when one sweeps so rapidly through resonance that either thermal equilibrium is not achieved or the adiabatic condition is not satisfied. The wiggles were treated theoretically by Jacobsohn and Wangsness.[7] For the conditions mentioned above, the nuclear moment fails to precess in step with the applied rf, and a beat due to the interference of these two separate frequencies is seen. Later, Torrey[8] analyzed a similar transient case that occurs when one establishes a nonequilibrium situation and then fixes the experimental parameters, including the strength and frequency of the rf field and the value of the polarizing field. Thus some transient effects were observed quite early, but they were not observed in the absence of an rf field as described by Bloch for the FID.

In October 1948, Russell Varian filed a patent application entitled 'Method and Means for Correlating Nuclear Properties of Atoms and Magnetic Fields'.[9] The patent describes a specific method for changing the orientation of the nuclear moments so that they form an angle with the magnetic field, usually the Earth's field. A polarizing field is established at an angle with respect to the field to be measured (which is usually the Earth's magnetic field). After a nuclear polarization is established, the polarizing field is quickly shut off, leaving the nuclear moments at an angle with the Earth's field. They then precess about the direction of the Earth's field and, in so doing, induce a voltage in a coil surrounding the sample. This coil is coupled to a sensitive amplifier, the output of which is connected to a means of measuring the precessional frequency, which is proportional to the Earth's magnetic field strength. In the original systems, a frequency counter was used to determine the frequency. A reed frequency meter, which is a crude Fourier analyzer, was used in a later portable magnetometer.

In the year 1949–50, Hahn performed a number of experiments that made use of the pulsed rf field methods suggested by Bloch. He used a combination of an inversion pulse and a rapid scan through the resonance region to measure the thermal relaxation time of water.[10a] Later he described the FID signals that follow a short pulse and developed the theory and experimental techniques of spin echo NMR. With the spin echo

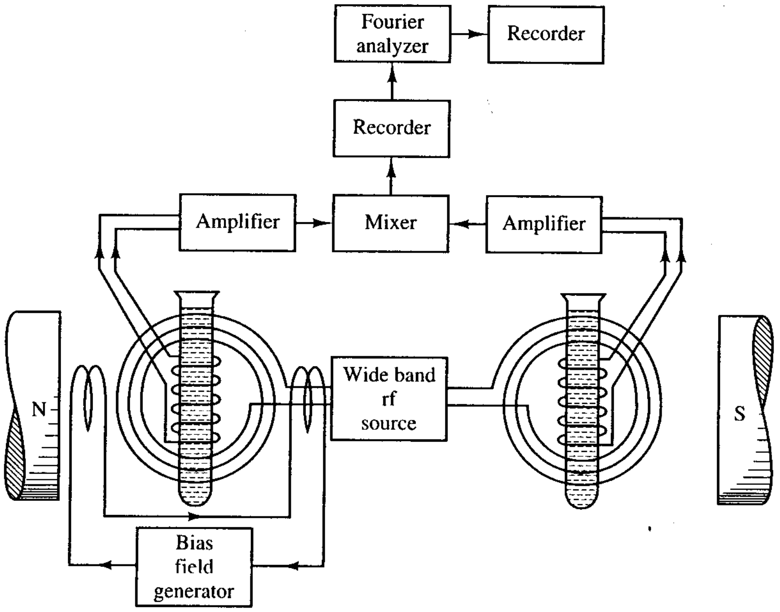

Figure 1 The FT NMR system described in the Russell Varian US Patent[12]

technique he measured the NMR relaxation times T_1 and T_2.[10b,c] Hahn and Maxwell analyzed the complex echo patterns found in molecules that contained spin-coupled chemical groups.[11]

In August 1956, Russell Varian filed a patent[12] which contained the major concepts of FT NMR as a method of increasing the sensitivity of NMR spectrometers. Here a wideband frequency source is used to excite simultaneously all the resonance lines in an NMR spectrum. After storing the responses, an FT analyzer is used to convert the response into a frequency spectrum. The system described in his patent is illustrated in Figure 1. It is stated in the patent that 'the wide band frequency source may comprise, for example, a pulse generator wherein the pulses are regulated to give Fourier components over the desired frequency range or a white noise source having the required bandwidth'. In this system he also provided a field/frequency control using a NMR reference sample. Signals from the analytical and reference samples are mixed together to obtain a signal at the difference frequency, thereby eliminating the effects of frequency or field drift. Two different Fourier analyzer systems are described: in one the signal is recorded on photographic film, and in the other it is recorded on magnetic tape. In the first system, the FT is performed by using the film as a diffraction grating in an optical spectrometer arrangement. The spectrum, i.e. the FT, is recorded on a second film by a beam of light that is diffracted by the image on the first film. After it has been developed, the second film is read with a photoelectric densitometer and recorded on a strip chart recorder. In the magnetic tape system the Fourier analysis is performed by playing the recorded signal to a mixer and sending the output through a low-pass filter and detector to the strip chart recorder. The mixer receives a reference signal from a variable-frequency oscillator. The frequency of this oscillator determines the frequency component of the output spectrum.

Because of their complexity, neither of these systems was built. However, the claims of the patent were sufficiently broad to cover practical systems that were developed later. From a reading of the patent it is obvious that Russell Varian had a clear understanding that the NMR response to a wideband source and the spectrum formed an FT pair. Before the patent issued in 1966, Lowe and Norberg[13] had also pointed out that the FID and spectrum formed an FT pair.

In the early 1960s, the need for greater sensitivity was growing. The increase in strength of the polarizing magnetic field was a help, as was the repetitive averaging of spectra by adding together many spectra in a computer of average transients (CAT) that became available about this time. The multiplex advantage, as suggested by the Varian patent, seemed to offer increased sensitivity without taking additional time to perform time averaging. In 1962, Anderson proposed a multichannel NMR spectrometer to make use of the multiplex advantage. He proposed using a chopper wheel to generate a band of frequencies which, after mixing with an offset frequency, could be applied to produce simultaneous resonance of the sample nuclei. The responses, after mixing with the same offset frequency, could be demodulated by the same chopper wheel and provide simultaneous multiple output signals in real time[14] (see also ***Early NMR Experiences and Experiments***). These output signals could be integrated to achieve the desired signal-to-noise ratio. Before the chopper wheel was put into operation, Anderson realized that a series of pulses would be a better way to achieve a band of discrete rf fields. After mixing, the response signals could be stored using a CAT and then Fourier transformed by a computer. This approach was even closer to the Varian patent. The necessary equipment was assembled and the idea successfully tested by Richard Ernst. In the early experiments Ernst and Anderson found a sensitivity enhancement of more than 10 in experiments using the same data acquisition time (Figure 2) (see ***Early NMR Experiences and Experiments***).[15]

The improvement in sensitivity provided by the FT technique, compared with the previous field or frequency scanned

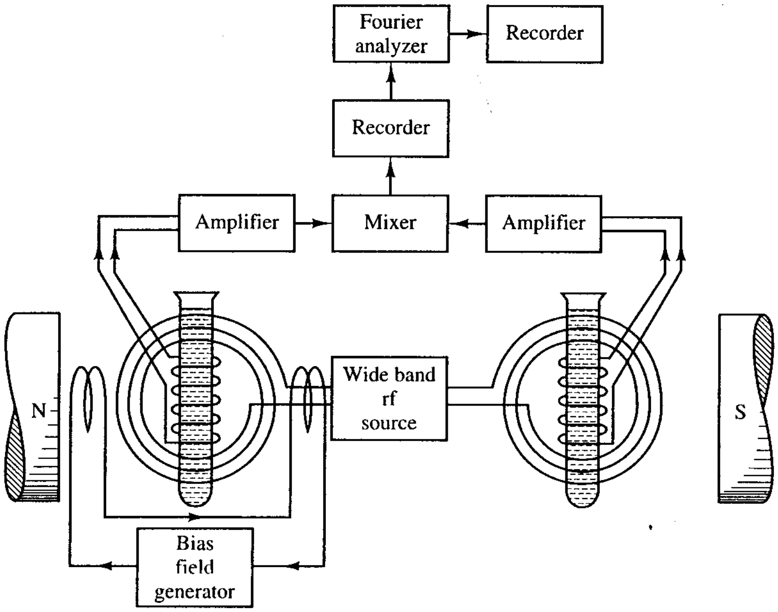

Figure 1 The FT NMR system described in the Russell Varian US Patent[12]

technique he measured the NMR relaxation times T_1 and T_2.[10b,c] Hahn and Maxwell analyzed the complex echo patterns found in molecules that contained spin-coupled chemical groups.[11]

In August 1956, Russell Varian filed a patent[12] which contained the major concepts of FT NMR as a method of increasing the sensitivity of NMR spectrometers. Here a wideband frequency source is used to excite simultaneously all the resonance lines in an NMR spectrum. After storing the responses, an FT analyzer is used to convert the response into a frequency spectrum. The system described in his patent is illustrated in Figure 1. It is stated in the patent that 'the wide band frequency source may comprise, for example, a pulse generator wherein the pulses are regulated to give Fourier components over the desired frequency range or a white noise source having the required bandwidth'. In this system he also provided a field/frequency control using a NMR reference sample. Signals from the analytical and reference samples are mixed together to obtain a signal at the difference frequency, thereby eliminating the effects of frequency or field drift. Two different Fourier analyzer systems are described: in one the signal is recorded on photographic film, and in the other it is recorded on magnetic tape. In the first system, the FT is performed by using the film as a diffraction grating in an optical spectrometer arrangement. The spectrum, i.e. the FT, is recorded on a second film by a beam of light that is diffracted by the image on the first film. After it has been developed, the second film is read with a photoelectric densitometer and recorded on a strip chart recorder. In the magnetic tape system the Fourier analysis is performed by playing the recorded signal to a mixer and sending the output through a low-pass filter and detector to the strip chart recorder. The mixer receives a reference signal from a variable-frequency oscillator. The frequency of this oscillator determines the frequency component of the output spectrum.

Because of their complexity, neither of these systems was built. However, the claims of the patent were sufficiently broad to cover practical systems that were developed later. From a reading of the patent it is obvious that Russell Varian had a clear understanding that the NMR response to a wideband source and the spectrum formed an FT pair. Before the patent issued in 1966, Lowe and Norberg[13] had also pointed out that the FID and spectrum formed an FT pair.

In the early 1960s, the need for greater sensitivity was growing. The increase in strength of the polarizing magnetic field was a help, as was the repetitive averaging of spectra by adding together many spectra in a computer of average transients (CAT) that became available about this time. The multiplex advantage, as suggested by the Varian patent, seemed to offer increased sensitivity without taking additional time to perform time averaging. In 1962, Anderson proposed a multichannel NMR spectrometer to make use of the multiplex advantage. He proposed using a chopper wheel to generate a band of frequencies which, after mixing with an offset frequency, could be applied to produce simultaneous resonance of the sample nuclei. The responses, after mixing with the same offset frequency, could be demodulated by the same chopper wheel and provide simultaneous multiple output signals in real time[14] (see also ***Early NMR Experiences and Experiments***). These output signals could be integrated to achieve the desired signal-to-noise ratio. Before the chopper wheel was put into operation, Anderson realized that a series of pulses would be a better way to achieve a band of discrete rf fields. After mixing, the response signals could be stored using a CAT and then Fourier transformed by a computer. This approach was even closer to the Varian patent. The necessary equipment was assembled and the idea successfully tested by Richard Ernst. In the early experiments Ernst and Anderson found a sensitivity enhancement of more than 10 in experiments using the same data acquisition time (Figure 2) (see ***Early NMR Experiences and Experiments***).[15]

The improvement in sensitivity provided by the FT technique, compared with the previous field or frequency scanned

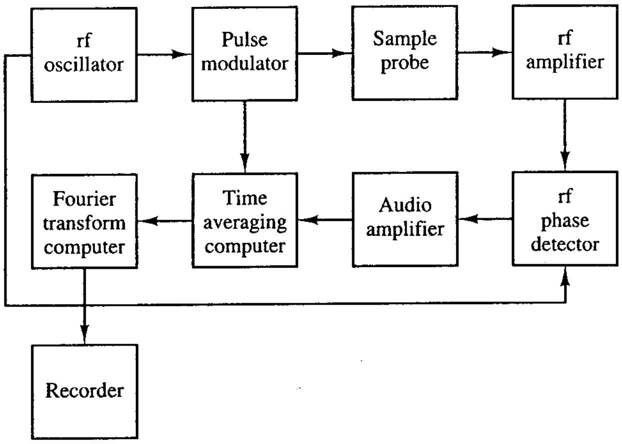

Figure 2 The FT NMR system described by Anderson and Ernst[15]

experiments, is determined primarily by the ratio of the spectrum width F and the linewidth of a single transition $\Delta = 1/\pi T_2$. The time taken to obtain a spectrum by an FT experiment yielding essentially the same signal-to-noise ratio is reduced by a factor of F/Δ. By signal averaging, the signal-to-noise ratio increase is proportional to the square root of the number of averaged spectra. Thus, to first order, the FT technique provides an increase in the signal-to-noise ratio by a factor of approximately $\sqrt{(F/\Delta)}$ for the same total data collection time. With the larger spectral widths arising from the greater magnetic field strengths of modern systems, the gain in the signal-to-noise ratio can be a factor of 100 or more for ^{13}C or ^{1}H experiments in liquid samples.

The use of a broadband noise source was demonstrated independently by Ernst[16] and Kaiser.[17] In these experiments a pseudorandom sequence was used to modulate the rf phase of the excitation to produce a wideband noise source. The advantage of the pseudorandom sequence is its predictable spectral properties and constant rf power. The rf power level is far lower than that required for pulsed FT; however, the simultaneous radiation and detection can lead to line broadening that is absent in pulsed FT spectroscopy.

In the rapid scan approach,[18] the rf field is quickly scanned through the NMR spectral region causing wiggles, as described above. The spectrum is corrected by a convolution with a scan of a single line made under identical conditions, or by one that is simulated on a computer. The signal from a single line resembles its FID, except that the frequency of the wiggles increases as the rf frequency is swept away from the resonance condition.

With flexible pulse programmers and frequency synthesizers that can be digitally controlled, an excitation function can be generated with virtually any spectral distribution by controlling the width, amplitude, phase, and perhaps frequency, of each pulse or pulse segment. This concept was originally applied to spin decoupling by Tomlinson and Hill,[19] and later used to produce composite pulses for the suppression of solvent lines and for other applications.[20]

In 1971, J. Jeener proposed that the Fourier transformation technique be extended into a second dimension, from which information could be extracted using additional pulses.[21] In 1974, Ernst and his group demonstrated the technique and showed how it could be particularly useful in analyzing large molecules.[22] A first pulse or group of pulses was used to establish a coherent nonequilibrium state in the spin system. The state of the spin system then evolves during a period called the 'evolution period'. A second pulse or pulse group then causes mixing of the evolved states. The detection period follows the mixing period. An FT is applied to the signals recorded during the detection period. Repeating the experiment for different evolution times yields a two-dimensional array of data. A second FT is applied with respect to this second time dimension, the evolution time, to produce a two-dimensional frequency spectrum.

Variations of the two-dimensional experiment can yield a wealth of information. Some of the more important applications involve tracing out the molecular structures by resolving spin couplings between protons, protons and ^{13}C, and between ^{13}C atoms. Overhauser types of experiment yield information on the conformation of polypeptides and small proteins. Overlapping lines are often resolved by spreading the spectrum out in a second or a third dimension.[23,24]

Magnetic resonance imaging (MRI) is a field in which FT techniques are essential. MRI began when Paul Lauterbur proposed the use of NMR for imaging in a manner analogous to the use of computerized tomography (CT) in X-ray imaging. Lauterbur's critical idea was to use magnetic field gradients, making the frequencies of the NMR resonance signals dependent upon the spatial position of the resonant nuclei.[25] A number of techniques developed by Hinshaw made use of the multiplex advantage of FT NMR. Generally, the techniques involved simultaneously detecting all the resonances in a line or plane with the spatial positions coded by magnetic field gradients, and later reconstructing by the back-projection used in CT.[26] In 1975, Ernst proposed a way of acquiring and reconstructing MRI data that was similar to the two-dimensional spectroscopic method.[27] A magnetic field gradient is applied during the evolution period between pulses, and an orthogonal gradient is applied during the detection period. By repeating the experiment a number of times, each time incrementing the duration of the evolution time, a series of responses is collected. Applying a double FT with respect to the different times yields a cross-sectional image. The method was readily extended to three dimensions. This Fourier imaging technique, and a modified form known as spin warp imaging,[28] is the most frequently used method of MRI.

Resonances from nuclei in solid samples are split and shifted by the static dipole–dipole coupling between nuclei and by quadrupole coupling of nuclei that have electric quadrupole moments. Because the splittings and shifts depend upon the orientation of the interaction with respect to the polarizing field, resonances in a polycrystalline sample are further broadened. As a result, the FID from nuclei in a solid can be very short, and instrumental limitations of finite rf pulse lengths and receiver recovery times limit its direct observation.

Spin echo techniques[10] can be used to overcome partially the problem of short FID transients that decay during the receiver dead time following the excitation pulse. The techniques are suitable for a polycrystalline material with strong dipole or quadrupole couplings. The basic spin echo technique uses two excitation pulses separated by a short time interval. The magnetization then rephases to form a dipolar echo[29] or quadrupolar echo.[30] At the echo peak the magnetization is rephased as at the start of the FID. Now, however, the signal is separated from any interfering rf pulses so that it may be recorded accurately. Fourier transformation of the second half of the echo produces the spectral response.

A number of techniques reduce line broadening, allowing the extraction of spectral information by FT methods. Magic angle spinning (MAS), introduced by Andrew et al.[31] and Lowe,[32] can reduce the dipole–dipole contribution to the linewidths in solids.[33] Combining MAS with heteronuclear decoupling and cross polarization[34] (CP MAS) provides high resolution capabilities for dilute nuclear spins such as those of ^{13}C.[35]

Repetitive pulse sequences have also been developed. These effectively average interactions that normally cause broadening of lines in solids. The spin system is subjected to a repetitive sequence of closely spaced pulses. The spin response is digitized once per cycle of the sequence, thus building up the equivalent of a single FID which is then transformed in the usual way to produce a spectrum.[36]

FT techniques have also been used in electron spin resonance (ESR), sometimes called electron paramagnetic resonance (EPR) spectroscopy. Generally, the electron FID signals are much shorter than the nuclear FID response found in liquids and solids; however, as the electronic equipment has improved, many of the multiple pulse and two-dimensional experiments commonly used in NMR have been applied to ESR.[37,38]

FT techniques have been applied to many other forms of spectroscopy, such as ion cyclotron resonance (ICR) mass spectroscopy, nuclear quadrupole resonance (NQR), EPR, dielectric spectroscopy, and microwave spectroscopy. Marshall has reviewed many of these techniques. The way in which FT methods have increased the sensitivity of these techniques is described below.[39]

3 THE MATHEMATICS OF THE FOURIER TRANSFORM

There are a number of different mathematical formulations of the FT and the inverse transform.[40] One pair is given by the equations:

$$F(\nu) = \int_{-\infty}^{\infty} f(t)\exp(-\mathrm{i}2\pi\nu t)\,\mathrm{d}t \qquad (1)$$

$$f(t) = \int_{-\infty}^{\infty} F(\nu)\exp(\mathrm{i}2\pi\nu t)\,\mathrm{d}\nu \qquad (2)$$

where $\mathrm{i} = \sqrt{-1}$, $f(t)$ is a function of time t, and $F(\nu)$ is a function of the frequency ν. The inverse transformation converts a frequency spectrum $F(\nu)$ back into the time domain $f(t)$.

The angular frequency $\omega = 2\pi\nu$ is often used for formal expressions yielding the transformation pair:

$$F(\omega) = \int_{-\infty}^{\infty} f(t)\exp(-\mathrm{i}\omega t)\,\mathrm{d}t \qquad (3)$$

and

$$f(t) = \frac{1}{2\pi}\int_{-\infty}^{\infty} F(\omega)\exp(\mathrm{i}\omega t)\,\mathrm{d}\omega \qquad (4)$$

Note that the expressions for $F(\omega)$ and $F(\nu)$ differ by 2π.

There are a number of properties or theorems that play a basic role in the application of FT pairs.[40] Some of the more useful ones are summarized below. By interchanging $F(\nu)$ and $f(t)$ and changing i to $-$i, the theorems also apply to the inverse transformations.

3.1 Similarity Theorem

If $f(t)$ has the FT $F(\nu)$, then $f(at)$ has the FT $|1/a|F(\nu/a)$.

This theorem illustrates that if the timescale is compressed by a factor of a ($a < 1$), the frequency scale expands by $1/a$, and, as it expands, the area of the spectrum remains constant.

3.2 Addition Theorem

If $f(t)$ and $g(t)$ have the FTs $F(\nu)$ and $G(\nu)$, respectively, then $f(t) + g(t)$ has the transform $F(\nu) + G(\nu)$.

This theorem illustrates that the FT transform is a linear transform and is suitable for dealing with linear problems. Although the NMR magnetization $\boldsymbol{M}$ does not respond linearly to the rf pulse, the subsequent FID motions are linear and the addition theorem applies.

3.3 Shift Theorem

If $f(t)$ has the FT $F(\nu)$, then $f(t - t_0)$ has the FT $\exp(-\mathrm{i}2\pi\nu t_0)F(\nu)$.

This theorem illustrates that a change in the time origin of the FID causes a frequency-dependent phase change in the resulting spectrum. Modern NMR spectrometers can correct for frequency-dependent phase errors in the spectrum.

3.4 Convolution Theorem

If $H(\nu)$ represents the convolution of the two functions $F(\nu)$ and $G(\nu)$, then its FT $h(t)$ can be expressed as the product of the two functions $f(t)$ and $g(t)$ where they are the FTs of $F(\nu)$ and $G(\nu)$, respectively.

The convolution operator is expressed as:

$$\hat{H}(\nu) = F(\nu) * G(\nu) = \int_{-\infty}^{\infty} F(\mu)G(\nu - \mu)\,\mathrm{d}\mu \qquad (5)$$

and the corresponding relationship for the FT of these quantities is $h(t) = f(t)g(t)$. This theorem is extremely useful in any filtering process that makes use of convolution. To achieve the maximum possible signal-to-noise ratio, it is necessary to use a matched filter, which is determined by the lineshape. The FID of a Lorentzian spectral line with a relaxation time T_2 corresponds to a decay envelope given by $\exp(-t/T_2)$. Thus to obtain a spectrum with the best possible signal-to-noise ratio, the FID is multiplied by $\exp(-t/T_2)$ before the FT is taken.

Other filter applications that can make use of the convolution theorem include: resolution enhancement, to narrow artificially the resonance lines; lineshape transformations (for example, to transform the Lorentzian lines to Gaussian lines which cut off faster with frequency); apodization of the FID to suppress or eliminate oscillating signal tails in the spectrum; and correction of instrumental distortions, perhaps caused by the limited receiver bandwidth. These processes are trivial when done in the time domain, as compared to performing a convolution in the frequency domain.[23]

3.5 Definite Integral

The definite integral of a function $F(\nu)$ from $-\infty$ to ∞ is equal to the value of its FT at the origin, $f(0)$.

$$f(0) = \int_{-\infty}^{\infty} F(\nu)\,\mathrm{d}\nu \tag{6a}$$

$$F(0) = \int_{-\infty}^{\infty} f(t)\,\mathrm{d}t \tag{6b}$$

This states that the initial value of a FID is equal to the area of its FT. With proper attention to the NMR phase adjustments, one can relate the initial value of the FID to the total area in the NMR spectrum.

3.6 Rayleigh's Theorem

The integral of the squared modulus of a function is equal to the integral of the squared modulus of its spectrum.

$$\int_{-\infty}^{\infty} |f(t)|^2\,\mathrm{d}t = \int_{-\infty}^{\infty} f(t)f^*(t)\,\mathrm{d}t = \int_{-\infty}^{\infty} F(\nu)F^*(\nu)\,\mathrm{d}\nu = \int_{-\infty}^{\infty} |F(\nu)|^2\,\mathrm{d}\nu \tag{7}$$

Here each integral represents the energy of the system. The term $|f(t)|^2$ has some interesting properties in that its value does not depend upon the origin or frequency offset of the transmitter.

3.7 The Sine and Cosine Transforms

The cosine transform $C(\nu)$ and sine transform $S(\nu)$ are obvious extensions of the standard FT:

$$C(\nu) = \int_{-\infty}^{\infty} f(t)\cos(2\pi\nu t)\,\mathrm{d}t \tag{8a}$$

$$S(\nu) = \int_{-\infty}^{\infty} f(t)\sin(2\pi\nu t)\,\mathrm{d}t \tag{8b}$$

It is useful to note that the cosine transform is symmetric about $\nu = 0$ and the sine transform is antisymmetric about $\nu = 0$. If $f(t)$ is real, then the real part of $F(\nu)$ is symmetric and the imaginary part antisymmetric about $\nu = 0$.

3.8 The Discrete Fourier Transform

For most NMR applications, the data have a finite time duration and are sampled and recorded at discrete time intervals. The discrete FT (DFT) is based on the use of periodic functions with period N so that $x(n) = x(n+kN)$, where n, N, and k are integers.[40,41] The DFT is defined within the limited region of what would be one period of the periodic function. In contrast to Fourier series, which may have an infinite number of terms, there are only N distinct complex exponentials used in the DFT. The DFT and inverse transform can be written as:

$$F(\nu_k) = \sum_{n=0}^{N-1} f(t_n)\exp(-\mathrm{i}2\pi kn/N) \tag{9}$$

$$f(t_n) = \frac{1}{N}\sum_{k=0}^{N-1} F(\nu_k)\exp(\mathrm{i}2\pi kn/N) \tag{10}$$

The normalizing factor $1/N$ arises from the equality:

$$\sum_{n=0}^{N-1} \exp(\mathrm{i}2\pi nk/N) = \begin{cases} N, & \text{for } k = mN,\ m \text{ an integer} \\ 0, & \text{otherwise} \end{cases} \tag{11}$$

In NMR, the FID signals are digitized at times $t_n = n\Delta\tau$, where $\Delta\tau$ is the time interval between successive analog-to-digital converter (ADC) samples, and n takes the N integer values from 0 to $N - 1$. The spectral frequencies ν_k measured in the rotating coordinate system extend from $-1/(2\Delta\tau)$ to $1/(2\Delta\tau)$, and have the values $\nu_k = k/(N\,\Delta\tau)$, where N is the total number of FID samples. In a single-channel system, k ranges from 0 to $N/2$, and in a quadrature system (discussed below) k ranges from $-N/2$ to $+N/2$. Modern computers and the fast FT (FFT) algorithms permit rapid computation of the DFT.[43,44]

4 THE BLOCH EQUATIONS

The FT NMR experiments that use rf pulses for excitation are treated in greater detail here, since they are the ones in greatest use today. A FID signal is stimulated by applying a short rf magnetic field pulse at right angles to the constant polarizing magnetic field. Following the conventional notation, the polarizing magnetic field is along the z axis and the rf magnetic field along the x axis. By increasing the phase of the rf drive frequency by 90°, the effective axis of the rf field is changed to lie along the y axis. Thus roles of the x- and y-axes are easily interchanged, thereby permitting experiments where the effective rf field can be applied in any direction in the xy plane.

The phenomenological equations of Bloch[5] and his development of the rotating coordinate system provide an easy way to describe the FT experiment and to resolve many questions regarding the optimization of experimental parameters. The equations in the laboratory system are:

$$\dot{M}_x = \gamma(M_yB_z - M_zB_y) - M_x/T_2 \tag{12a}$$

$$\dot{M}_y = \gamma(M_zB_x - M_xB_z) - M_y/T_2 \tag{12b}$$

$$\dot{M}_z = \gamma(M_xB_y - M_yB_x) - (M_z - M_0)/T_1 \tag{12c}$$

where M is the magnetization vector, $\dot{M}$ is the time derivative of M, and B is the applied magnetic field vector, with the subscripts indicating the particular components. With only a polarizing field B_z and no other magnetic field components, a solution of these equations is:

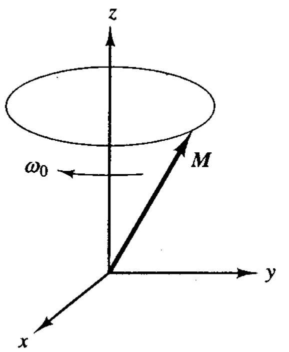

Figure 3 Precessing magnetization in the presence of a constant field B_z along the z axis

$$M_x = M_T \cos(\omega_0 t + \phi) \exp(-t/T_2) \quad (13)$$

$$M_y = M_T \sin(\omega_0 t + \phi) \exp(-t/T_2) \quad (14a)$$

$$M_z = M_0 + M_L \exp(-t/T_1) \quad (14b)$$

where $\omega_0 = -\gamma B_z$, and M_T is the total transverse magnetization. In a right-handed coordinate system, a positive value of γ yields a negative value of ω_0. These equations describe a magnetization vector precessing about the magnetic field axis at an angular frequency of ω_0, as shown in Figure 3. With the positive z axis taken in the direction of the magnetic field B_z, the sign of ω_0 is the same as the sign of $-\gamma$. The xy component of the magnetization decays toward zero with a time constant T_2, and the z component of magnetization approaches M_0 with a time constant T_1.

Using complex notation $f(t) = M^+ = M_x + iM_y = M_T \exp(i\omega_0 t + i\phi - t/T_2)$ and inserting it into equation (3) yields

$$\begin{aligned} F(\omega) &= M_T \exp(i\phi) \int_0^\infty \exp[i(\omega_0 - \omega)t - t/T_2]\,dt \\ &= M_T \exp(i\phi) \frac{1/T_2 + i(\omega_0 - \omega)}{(\omega_0 - \omega)^2 + (1/T_2)^2} \end{aligned} \quad (15)$$

Choosing the transverse magnetization M_T to be aligned along the x axis at time $t = 0$ corresponds to the phase $\phi = 0$. In this case the real part of $F(\omega)$ corresponds to the absorption signal $a(\Delta\omega)$, and the imaginary part corresponds to the dispersion signal $d(\Delta\omega)$ where

$$a(\Delta\omega) = M_T \frac{1/T_2}{(\Delta\omega)^2 + (1/T_2)^2} \quad (16a)$$

$$d(\Delta\omega) = M_T \frac{\Delta\omega}{(\Delta\omega)^2 + (1/T_2)^2} \quad (16b)$$

with the frequency offset $\Delta\omega = \omega_0 - \omega$.

4.1 The Rotating Coordinate Frame

The concept of the rotating coordinate frame can be helpful when visualizing the magnetization during the time for which an rf pulse is applied. In most FT experiments the pulse length τ is short compared with T_1 and T_2 so that, while the pulse is being applied, the terms in equations (12a)–(12c) containing T_1 and T_2 can be safely omitted. After the termination of the pulse, the solutions for the magnetization M are again given by equations (13), (14a) and (14b) with new values for M_T, M_L, and ϕ. It may be more useful to express the magnetization M in the rotating coordinate frame even after the termination of the pulse. In most spectrometer systems the signals are mixed with the transmitter frequency, so that the frequencies of the signals at the output of the mixer correspond to those of the rotating frame.

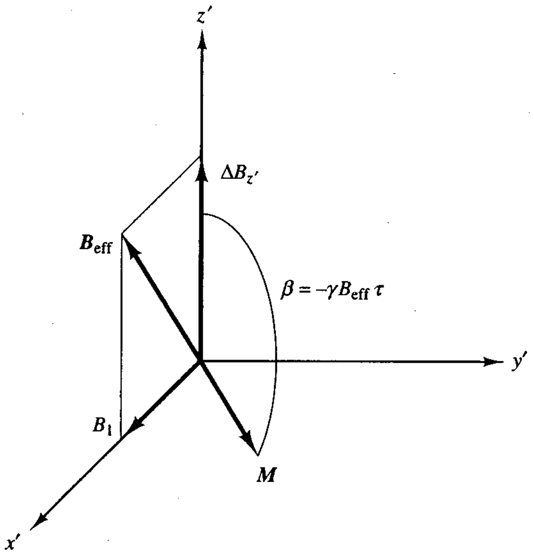

Figure 4 Magnetization precessing about the effective field B_{eff} in the coordinate frame with axes x', y' and z' rotating with the rf field. The field B_{eff} is the vector sum of the rf field B_1 along the x' axis and the offset field ΔB_z along the $z' = z$ axis

The rf pulse is normally described as a linearly oscillating field $2B_1 \cos(\omega_{rf} t + \psi)$. This field is equivalent to two counter-rotating fields, each with strength B_1. Only the component that rotates in the same sense as the magnetization is effective in perturbing the nuclear spins. With $|B_1/B_z| << 1$ the counter-rotating component is safely ignored. Thus in the coordinate frame that rotates with the angular frequency ω_{rf}, the perturbing rf field has static components $B_{x'} = B_1 \cos \psi$ and $B_{y'} = B_1 \sin \phi$. By selecting the field $\Delta B_{z'} = B_z + \omega_{rf}/\gamma = -(\omega_0 - \omega_{rf})/\gamma$, the Bloch equations in the rotating system are identical to those of the static system. The solution to the equations is obvious. The magnetization in the rotating frame just precesses about the effective field of magnitude $B_{eff} = \sqrt{(\Delta B_{z'}^2 + B_1^2)}$ at the frequency $\omega' = -\gamma B_{eff}$, so that at the end of a pulse of length τ the magnetization M has been rotated through an angle $\beta = \gamma B_{eff}\tau$. The fields in the rotating coordinate system with $\phi = 0$ are illustrated in Figure 4.

If the rf frequency corresponds to the resonant frequency of the NMR line, then $\Delta B_{z'} = 0$ and the angle of rotation during an rf pulse $\beta = \gamma B_1 \tau$. If initially the magnetization is at equilibrium, that is directed along the z axis with $M_z = M_0$, then an rf pulse with $\beta = \pi/2$ (90° pulse) will rotate the magnetization from along the z axis to the xy plane ($z = 0$), resulting in the maximum FID signal. The FT of this signal produces a real and an imaginary output. By selecting a combination of these two outputs, one can display either the absorption or dispersion mode NMR lines.

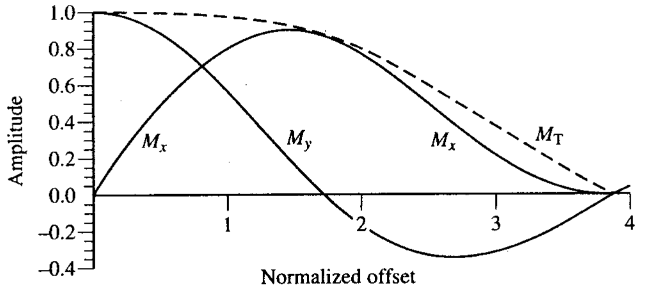

Figure 5 Plot of M_x, M_y, and M_T versus the normalized offset $[(\omega_o - \omega_{rf})/(-\gamma B_1)] = \Delta B_{z'}/B_1$. At an offset $\Delta B_{z'} = B_1$, the magnetization M_x is decreased by over 40% while the total magnetization $M_T = \sqrt{[(M_x)^2 + (M_y)^2]}$ is decreased by about 2%

To calculate the rotation of off-resonant lines, the magnetization is assumed initially to be aligned along the $z' = z$ axis. The rf field B_1 is along the x' axis, and the offset field $\Delta B_{z'}$ along the z' axis of the coordinate frame rotating at the angular frequency ω_{rf}. The total field in this rotating coordinate system is the vector addition of ΔB_z and B_1 to yield $\boldsymbol{B}_{eff}$ along the z'' axis, which makes an angle θ with respect to the z' axis (Figure 4). During the rf pulse, the magnetization, initially along z', rotates about z'' through an angle $\beta = -\gamma B_{eff}\tau$. At the end of the rf pulse the magnetization in this tilted rotating coordinate system has the following values, as can be deduced with the aid of Figure 4:

$$M_{x''} = -M_0 \sin\theta \cos\beta \tag{17a}$$

$$M_{y''} = M_0 \sin\theta \sin\beta \tag{17b}$$

$$M_{z''} = M_0 \cos\theta \tag{17c}$$

and expressing these values in the rotating coordinate frame yields:

$$M_{x'} = M_{x''} \cos\theta + M_{z''} \sin\theta = M_0 \sin\theta \cos\theta (1 - \cos\beta) \tag{18a}$$

$$M_{y'} = M_{y''} = M_0 \sin\theta \sin\beta \tag{18b}$$

$$M_{z'} = M_{z''} \cos\theta - M_{x''} \sin\theta = M_0 (\cos^2\theta + \sin^2\theta \cos\beta) \tag{18c}$$

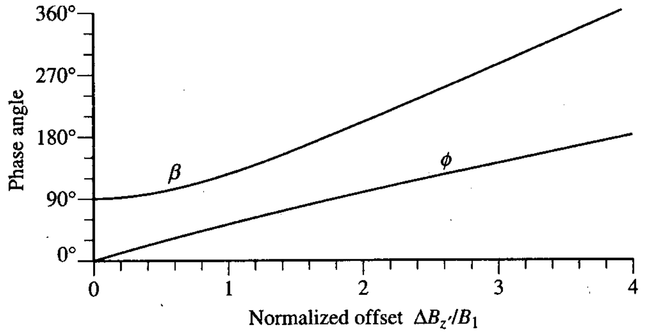

Figure 6 The phase angle ϕ and nutation angle β versus the normalized offset $\Delta B_{z'}/B_1$

The dependence of the signal amplitude as a function of the field offset $\Delta B_z/B_1$ is shown in Figure 5. The field strength B_1 has been selected by letting $\gamma B_1 \tau = \pi/2$, so the NMR lines near the rf ω_{rf} produce the maximum amplitude. The in-phase signals M_y and the quadrature phase signals M_x are plotted. By tracking the phase adjustment over the spectrum, one can expect to obtain an absorption or dispersion signal equal to the total transverse amplitude of the magnetization M_T. The phase shift $\phi = \arctan(M_x/M_y)$ and the total pulse rotation angle β are shown in Figure 6. It can be seen that a linear correction of the phase shift will compensate fairly closely for the frequency dependent phase shift over the frequency range comparable with the rf field strength $\gamma B_1/2\pi$.

As can be seen in Figure 5, the transverse magnetization vanishes when the normalized offset equals 3.87. Redfield and Gupta[45] proposed that strong solvent lines could be suppressed by adjusting their resonance to correspond to this offset. There are a number of composite pulse patterns that can be used for solvent suppression and to extend further the useful frequency range for a given pulse power.[20,46]

5 THE FOURIER TRANSFORM SPECTROMETER ELECTRONICS

A block diagram of an early FT NMR spectrometer is shown in Figure 2. In this system the transmitter frequency is normally adjusted to be just beyond one edge of the NMR spectral region. After mixing, the received signal and transmitter frequency are sent through a bandpass filter and then digitized and stored in the digital memory of a computer. A complex DFT is performed to obtain the output spectrum. A phase adjustment that provides a means of selecting the proper ratio of real and imaginary outputs of the DFT enables one to obtain a pure absorption or dispersion mode spectrum.[15]

5.1 Required Pulse Power

For proton resonance the typical value of the rf pulse amplitude is 25 kHz (5.9×10^{-4} T) for 10 μs to produce a 90° pulse. This takes a peak power of about 25 W at 600 MHz. This is sufficient to cover a spectrum width of about 25 kHz, which is quite adequate for proton spectra which have a spectral range of about 10 ppm. Carbon-13 is more of a problem with a spectral range of about 200 ppm and a smaller magnetic moment. At 14.1 T the width of the carbon spectral range is about 30 kHz, requiring a peak rf field strength of 28×10^{-4} T at 150 MHz. This takes a power of about 250 W at the 150 MHz operating frequency.

5.2 Quadrature System

The single-channel system suffers from several drawbacks that are overcome in dual channel or quadrature systems. One problem is that noise from both sides of the transmitter frequency is mixed with the signal frequency and contributes to the output noise. The quadrature system provides a $\sqrt{2}$ increase in sensitivity by eliminating the unwanted sideband noise. Another advantage is the more efficient use of rf pulse power gained by placing the rf at the center of the spectrum.[47] A block diagram of a quadrature system is shown in Figure 7.

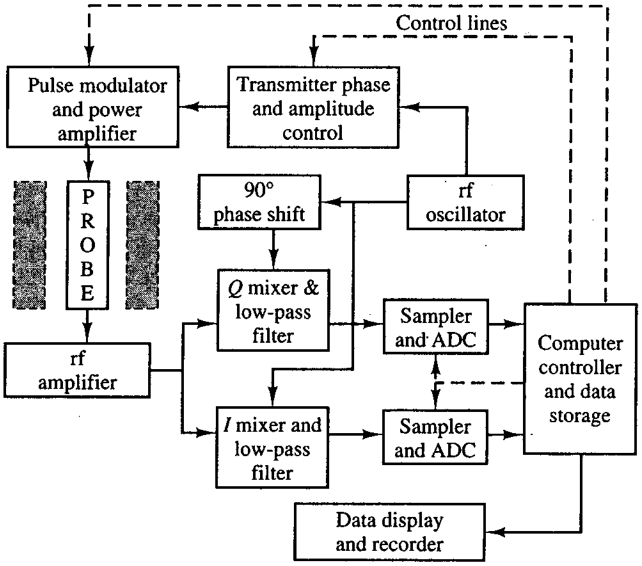

Figure 7 Block diagram of the electronics of an FT NMR spectrometer

The single sideband operation is obtained by splitting the receiver signals into two channels, and mixing one with a reference frequency that is in phase with the transmitter frequency, and mixing the other with a reference frequency in quadrature with the transmitter frequency.[47] After low-pass filtering, each of these two channels is digitized and stored in digital memory. The FT is applied separately to the signals in each of the two channels leading to four frequency domain signals. These can then be combined to select signals from either side of the transmitter frequency and, in addition, to display the desired absorption or dispersion mode spectrum (see Figure 7).

The low-pass filters are designed to cut out all frequencies greater than $1/(2\Delta\tau)$. The bandwidth of the system extends from $f_{\mathrm{rf}} - 1/(2\Delta\tau)$ to $f_{\mathrm{rf}} + 1/(2\Delta\tau)$. Any NMR signals, or noise that is generated outside of this frequency range, to the extent they are not filtered out by the low-pass filter, are present in the output. This process is called 'aliasing'. Aliased signals can usually be detected by their different appearance since their higher frequency experiences a greater phase shift in the low-pass filter.

5.3 Phase Cycling

One problem that can occur in quadrature detection systems is the incomplete separation between the NMR signals on the two sides of the transmitter frequency. This can happen if the in-phase and quadrature phase channels are not adequately matched. The gains of the two channels must be nearly identical and the two mixers must receive reference signals that have a precise 90° phase difference. In the case of a mismatch, when the signals from the two channels are combined the cancellation of the unwanted sideband is not complete. Phase cycling of the transmitter frequency is a way to get around this problem. Phase cycling is done by shifting the transmitter phase by 90° on each successive readout pulse and routing the data with the correct sign to each of the four memory channels. After a first pulse the real and imaginary data of the I mixer go to memory locations 1 and 2, and the data of the Q mixer go to memory channels 3 and 4. The phase of the next transmitter pulse is increased by 90° and the roles of the I and Q mixers are interchanged. After this pulse, the data from mixer I go to memory channels 3 and 4, taking into account the correct sign, and similarly the data of mixer Q go to memory locations 1 and 2. During the third pulse, the transmitter phase is shifted by 180° compared with the first pulse, and the outputs of the I and Q mixers go to the same locations as in the first pulse, except for a sign change. After the fourth pulse, the routing configuration is identical to that of the first pulse.[48] This process has been called CYCLOPS by Hoult and Richards.[49] With suitable spectrometer programming the task can be performed automatically. After a sufficient number of phase cycles have been completed, the data are Fourier transformed and combined in the usual way to give the complete spectrum.

5.4 Digitization Rates and Number of Data Points

When taking the data, a choice must be made on the digitization rate $1/\Delta\tau$, and the total number of data points taken N. The Nyquist criterion relates the highest frequency at which nonredundant data occur in the spectrum. In a single-channel system the transmitter frequency is normally placed to one side of the NMR spectral region that is to be investigated, and so the output of the mixer contains signal frequencies from 0 to $0.5/\Delta\tau$. In a quadrature system, twice as many data points are obtained and the frequencies on the two sides of the transmitter frequency can be separated, giving spectral data from $-0.5/\Delta\tau$ to $+0.5/\Delta\tau$. The total time spent in obtaining the FID data $T = N\Delta\tau$ determines the density of data points in the spectrum. Stopping the data-taking process before the FID has decayed sufficiently produces 'truncation wiggles' in the spectrum (Figure 8). The truncation process is equivalent to multiplying a complete FID by a square wave of duration T. In the fre-

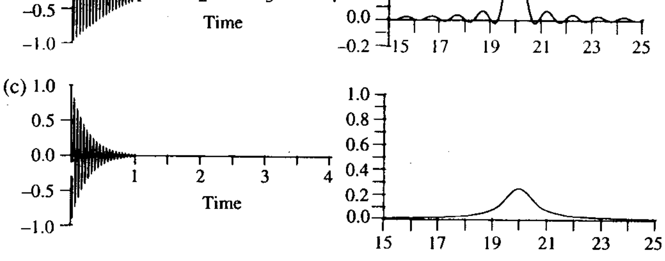

Figure 8 Simulated FID with T_2 = 1 s on the left and the corresponding FT on the right. (a) The full FID and its FT. (b) The FID truncated after 1 s and its FT. (c) The truncated FID, apodized with the function $\exp(-t/T)$ with T = 0.33 s, and its FT. In order to plot smoothed spectra, all FIDs were zero-filled before taking the FT

quency domain this is equivalent to a convolution of the NMR spectrum with the spectrum of a square wave of width T. This problem can be avoided by taking more FID data points, N, by increasing $\Delta\tau$, or by applying a windowing function, as discussed in the next section.

5.5 Apodization Windows

To prevent a sharp discontinuity at the end of the FID, it can be multiplied by a window function that goes smoothly toward zero at the end of the FID. One such function is $\exp(-t_n/T^*)$. As mentioned above, a matched filter with the value $T^* = T_2$, goes at least part way and provides a reduction in truncation wiggles. Making T^* even smaller will further reduce the truncation wiggles; however, there is a penalty of some loss in resolution. The smoothing and loss of resolution is apparent in the illustration at the bottom of Figure 8. Another common window function is the Hanning apodization which has the form $h(t_n) = 0.5[1 + \cos(\pi t_n/T)]$. Apodization may be combined with resolution enhancement by using a function such as $0.5[1 + \cos(\pi t_n/T)]\exp(2\pi t_n/T_2)$. A number of other window functions have been used.[23]

5.6 Zero Filling

As was mentioned above, by extending the time used to record the FID, the resolution can be improved at the expense the signal-to-noise ratio. Extending the data collection of the FID after it has decayed nearly to zero will increase the noise contribution more than the signal contribution. Zero filling is the process of inserting zeros in the data field at the end of the FID in order to extend artificially the duration T. With N real FID data points one obtains $N/2$ independent complex Fourier coefficients. In general, the real and imaginary data points in the spectrum are independent. Because of causality and a Hilbert transform relationship (sometimes called the 'Kramers–Krönig relationship') between the absorption and dispersion mode signals, one can obtain N absorption data points and N dispersion data points where now each contains the full information available from the FID. Bartholdi and Ernst[50] have shown that this can be achieved by appending N zeros to the FID data field before making the FT. Appending $(2n - 1)N$ zeros to the FID, with $n > 1$, will provide an additional interpolation of points in the spectrum, thus giving a spectrum which looks smoother but contains no further information.

5.7 Linear Prediction

It may be necessary or desirable to truncate the FID before it has substantially decayed, leading to truncation wiggles. Another problem is that it may not be possible to obtain the first few data points of an FID due to the dead time of the receiver or some other reason. Linear prediction is a process that extrapolates the data already contained in the FID in order to obtain a best guess of points beyond the range of the data, either before the first data point or after the last data point. The FID can be modeled using an arbitrary number of exponentially decaying sinusoidal waves to represent the contributions from the various NMR lines. Each line can be represented by an initial amplitude, decay time constant, frequency, and phase. After determining the best fit to the model, the model can be used to calculate additional points that may be missing before the start of the FID data or beyond the end of the truncated FID. The technique has been particularly useful in straightening out the baseline of a spectrum that was made from a delayed acquisition of the FID. It can also be used for resolution enhancement and smoothing of the data.[51]

The maximum entropy method is sometimes used to obtain the best fit of data to amplitude and frequency parameters. This method of fitting the data to a model has shown encouraging results; however, the lengthy computation required has prevented its wide acceptance.[52]

6 RELATED ARTICLES

Early NMR Experiences and Experiments; COSY Two-Dimensional Experiments; Double Resonance; Multidimensional Spectroscopy: Concepts; Probes for High Resolution; Selective Hartmann–Hahn Transfer in Liquids.

7 REFERENCES

1. A. A. Michelson, *Am. J. Sci.*, 1881, **22**, 120; *Phil. Mag. Ser.* 5, 1891, **31**, 256, 338; 1892, **34**, 280; 'Light Waves and Their Uses', University of Chicago Press, Chicago, IL, 1907.
2. P. Fellgett, *J. Phys. Radium*, 1958, **19**, 187; *J. Phys. (Paris)*, 1967, **28**, C2-165.
3. E. M. Purcell, H. C. Torrey, and R. V. Pound, *Phys. Rev.*, 1946, **69**, 37.
4. F. Bloch, W. W. Hansen, and M. Packard, *Phys. Rev.*, 1946, **69**, 127.
5. F. Bloch, *Phys. Rev.*, 1946, **70**, 460.
6. F. Bloch and W. W. Hansen, US Patent 2 561 489, filed 23 December 1946, issued 24 July 1951; reissued as US Patent 23 950, issued 22 February 1955.
7. B. A. Jacobsohn and R. K. Wangsness, *Phys. Rev.*, 1948, **73**, 942.
8. H. C. Torrey, *Phys. Rev.*, 1949, **76**, 1059.
9. R. H. Varian, US Patent 2 561 490, filed 28 October 1948, issued 24 July 1951; reissued as US Patent Re 23 769, issued 12 January 1954.
10. (a) E. L. Hahn, *Phys. Rev.*, 1949, **76**, 145; (b) 1950, **77**, 297; (c) 1950, **80**, 580.
11. E. L. Hahn and D. E. Maxwell, *Phys. Rev.*, 1952, **88**, 1070.
12. R. H. Varian, US Patent 3 287 629, filed 29 August 1956, issued 22 November 1966.
13. I. J. Lowe and R. E. Norberg, *Phys. Rev.*, 1957, **107**, 46.
14. W. A. Anderson, *Radiol. Today*, 1992, **9**, 1.
15. R. R. Ernst and W. A. Anderson, *Rev. Sci. Instrum.*, 1966, **37**, 93; W. A. Anderson and R. R. Ernst, US Patent 3 475 680, filed 26 May 1965, issued 28 October 1969.
16. R. R. Ernst, *J. Magn. Reson.*, 1970, **3**, 10.
17. R. Kaiser, *J. Magn. Reson.*, 1970, **3**, 28.
18. J. Dadok and R. F. Sprechen, *J. Magn. Reson.*, 1974, **13**, 243; R. K. Gupta, J. A. Ferretti, and E. D. Becker, *J. Magn. Reson.*, 1974, **13**, 275; J. A. Ferretti and R. R. Ernst, *J. Chem. Phys.*, 1976, **65**, 4283.
19. B. L. Tomlinson and H. D. W. Hill, *J. Chem. Phys.*, 1973, **59**, 1775.
20. M. H. Levitt and R. Freeman, *J. Magn. Reson.*, 1979, **33**, 473; M. H. Levitt, *Prog. NMR Spectrosc.*, 1986, **18**, 61.
21. J. Jeneer, Ampere Summer School, Basko Polje, Yugoslavia, 1971.
22. W. P. Aue, E. Bartholdi, and R. R. Ernst, *J. Chem Phys.*, 1976, **64**, 2229; R. R. Ernst, US Patent 4 134 058, filed 28 November

1977, issued 9 January 1979; US Patent 4168462, filed 5 June 1978, issued 18 September 1979.

23. R. R. Ernst, G. Bodenhausen, and A. Wokaun, 'Principles of Nuclear Magnetic Resonance in One and Two Dimensions', Clarenon, Oxford, 1987, Chaps. 4 and 6–9.
24. A. E. Derome, 'Modern NMR Techniques for Chemistry Research', Pergamon, Oxford, 1987, Chaps. 8–10; D. Shaw, 'Fourier Transform NMR Spectroscopy', 2nd edn, Elsevier, Amsterdam, 1984, Chap. 10.
25. P. C. Lauterbur,. *Bull. Am. Phys Soc.*, 1972, **18**, 86; *Nature*, 1973, **242**, 190.
26. W. S. Hinshaw, *J. Appl. Phys.*, 1976, **47**, 3709; H. R. Brooker and W. S. Hinshaw, *J. Magn. Reson.*, 1978, **30**, 129.
27. A. Kumar, D. Welti, and R. R. Ernst, *Naturwissenschaffe*, 1975, **62**, 34; A. Kumar, D. Welti, and R. R. Ernst, *J. Magn. Reson.*, 1975, **18**, 69; R. Ernst, US Patent 4070611, filed 13 April 1977, issued 24 January 1978.
28. W. A. Edelstein, J. M. S. Hutchinson, G. Johnson, and T. W. Redpath, *Phys. Med. Biol.*, 1980, **25**, 751; G. Johnson, J. M. S. Hutchinson, T. W. Redpath, and L. M. Eastwood, *J. Magn. Reson.*, 1983, **54**, 374.
29. P. Mansfield and D. Ware, *Phys. Lett.*, 1966, **22**, 133.
30. M. Bloom, J. H. Davis, and M. I. Valic, *Can. J. Phys.*, 1980, **58**, 1510.
31. E. R. Andrew, A. Bradbury, and R. G. Eades, *Arch. Sci.*, 1958, **11**, 223.
32. I. J. Lowe, *Phys. Rev. Lett.*, 1959, **2**, 258.
33. M. M. Maricq and J. S. Waugh, *J. Chem Phys.*, 1979, **70**, 3300; D. Muller, W. Gessner, H. J. Behrens, and G. Scheler, *Chem. Phys. Lett.*, 1981, **79**, 59.
34. S. R. Hartmann and E. L. Hahn, *Phys. Rev.*, 1962, **128**, 2042; A. Pines, M. G. Gibby, and J. S. Waugh, *Chem. Phys.*, 1973, **59**, 569.
35. J. Schaefer and E. O. Stejskal, *J. Am. Chem. Soc.*, 1976, **98**, 1031.
36. J. S. Waugh, L. M. Huber, and U. Haeberlen, *Phys. Rev. Lett.*, 1968, **20**, 180; U. Haeberlen, *Adv. Magn. Reson.*, 1976, (Suppl 1), Chaps. 4–6; B. C. Gerstein and C. R. Dybowski, 'Transient Techniques in NMR of Solids, An Introduction to Theory and Practice', Academic, Orlando, FL, 1985, Chaps. 5 and 6; E. O. Stejskal and J. D. Memory, 'High Resolution NMR in the Solid State', Oxford University Press, New York, chap. IID.
37. L. Kevan and M. Bowman, 'Modern Pulsed and Continuous-Wave Electron Spin Resonance', Wiley, New York, 1990; G. L. Mullhauser and J. H. Freed, *J. Chem. Phys.*, 1984, **81**, 37; T. Prisner, O. Dobbert, K. P. Dinse, and H. van Willigen, *J. Am. Chem. Soc.*, 1988, **110**, 1622.
38. S. Lee, B. R. Patyal, and J. H. Freed, *J. Chem. Phys.*, 1993, **98**, 3665.
39. A. G. Marshall, (ed.), 'Fourier, Hadamard, and Hilbert Transforms in Chemistry', Plenum, New York, 1982.
40. R. Bracewell, 'The Fourier Transform and Its Applications', McGraw Hill, New York, 1965, Chaps 6–8.
41. A. V. Oppenheim and R. W. Schafer, 'Digital Signal Processing', Prentice-Hall, Englewood Cliffs, NJ, 1975.
42. W. T. Cochran, J. W. Cooley, D. L. Favin, H. D. Helms, R. A. Kaenel, W. W. Lang, G. C. Maling, D. E. Nelson, C. M. Rader, and P. D. Welch, *Proc. IEEE*, 1967, **55**, 1664.
43. J. W. Cooley and J. W. Tukey, *Math. Comput.*, 1965, **19**, 297; B. Gold and C. Rader, 'Digital Processing of Signals', McGraw-Hill, New York, 1969; R. C. Singleton, *IEEE Trans. Audio Electroacoustics*, 1967, AU-15, 91.
44. For a short history of FFT algorithms see: J. W. Cooley and P. A. Welch, *Proc. IEEE*, 1967, **55**, 1675.
45. A. G. Redfield and R. K. Gupta, *J. Chem. Phys.*, 1971, **54**, 1418.
46. R. Freeman, S. P. Kempsell, and M. H. Levitt, *J. Magn. Reson.*, 1980, **38**, 453; M. H. Levitt, *J. Magn. Reson.*, 1982, **48**, 234; M. H. Levitt and R. R. Ernst, *J. Magn. Reson.*, 1983, **55**, 247.
47. R. R. Ernst, US Patent 3501691, filed 8 May 1968, issued 17 March 1970.
48. E. O. Stejkal and J. Schaefer, *J. Magn. Reson.*, 1974, **14**, 160.
49. D. Hoult and R. E. Richards, *Proc. R. Soc. (London), Ser. A*, 1975, **344**, 311.
50. E. Bartholdi and R. R. Ernst, *J. Mag. Reson.*, 1973, **11**, 9.
51. H. Barkhuijsen, R. de Beer, W. M. M. J. Bovée, and S. van Ormondt, *J. Magn. Reson.*, 1985, **61**, 465; C. F. Tirendi and J. F. Martin, *J. Magn. Reson.*, 1989, **81**, 557; J. F. Martin and C. F. Toremdo, *J. Magn. Reson.*, 1989, **82**, 392; D. Marion and A. D. Bax, *J. Magn. Reson.*, 1989, **83**, 205.
52. S. Sibisi, *Nature (London)*, 1983, **301**, 134; S. Sibisi, J. Skilling, R. G. Brerenton, E. D. Laue and J. Staunton, *Nature (London)*, 1984, **311**, 446; P. J. Hore, *J. Magn. Reson.*, 1985, **62**, 561; D. S. Stephenson, *Prog. NMR Spectrosc.*, 1988, **20**, 515.

Biographical Sketch

W. A. Anderson. *b* 1928. B.S., 1950, Ph.D., 1955, Stanford, CA, USA Ph.D. work under Prof. Felix Bloch on NMR. Special Assistant to the Director General of CERN, Geneva, Switzerland, 1955–56. Varian Associates, Palo Alto, CA, USA, 1955–present: Instrument Division Research Group, 1955–63; Director of Research, Instrument Division, 1963–72; Director of Systems & Techniques Laboratory, Varian Corporate Research, 1972–87; Principal Scientist, 1987–present; Varian Fellow, 1988–present. Approx. 40 publications and 40 issued US Patents.